Classification: Biological Sciences, Neuroscience

Towards Discovery Science of Human Brain Function: The '1000 Connectomes' Project

Bharat B. Biswal[1], Maarten Mennes[2], Xi-Nian Zuo[2], Suril Gohel[1], Clare Kelly[2], Steve M. Smith[3], Christian F. Beckmann[3], Jonathan S. Adelstein[2], Randy L. Buckner[4], Stan Colcombe[5], Anne-Marie Dogonowski[6], Monique Ernst[7], Damien Fair[8], Michelle Hampson[9], Matthew J. Hoptman[10], James S. Hyde[11], Vesa J. Kiviniemi[12], Rolf Kötter[13], Shi-Jiang Li[14], Ching-Po Lin[15], Mark J. Lowe[16], Clare Mackay[3], David J. Madden[17], Kristoffer H. Madsen[6], Daniel S. Margulies[18], Helen S. Mayberg[19], Katie McMahon[20], Christopher S. Monk[21], Stewart H. Mostofsky[22], James J. Pekar[23], Scott J. Peltier[24], Steven E. Petersen[25], Valentin Riedl[26], Serge A. R. B. Rombouts[27], Bart Rypma[28], Bradley L. Schlaggar[29], Sein Schmidt[30], Rachael D. Seidler[31], Greg Siegle[32], Christian Sorg[33], Gao-Jun Teng[34], Juha Veijola[35], Arno Villringer[36], Martin Walter[37], Lihong Wang[17], Xu-Chu Weng[38], Susan Whitfield-Gabrieli[39], Peter Williamson[40], Christian Windischberger[41], Yu-Feng Zang[42], Hong-Ying Zhang[34], F. Xavier Castellanos[2], Michael P. Milham[2]

[1] Department of Radiology, UMDNJ New Jersey Medical School, Newark, NJ 07103, USA

[2] Phyllis Green and Randolph Cowen Institute for Pediatric Neuroscience, New York University Child Study Center, NYU Langone Medical Center, New York, NY 10016, USA

[3] FMRIB Centre, University Oxford, Oxford OX3 9DU, UK

[4] Department of Psychology, Center for Brain Science, Harvard University, Cambridge, MA 02138, USA

[5] School of Psychology, University of Wales, Bangor, United Kingdom

[6] Department of MR, Section 340, Danish Research Center for Magnetic Resonance, DK-2650 Hvidovre, Denmark

[7] Mood and Anxiety Disorders Program, National Institute of Mental Health/National Institutes of Health, Department of Health and Human Services, Bethesda, MD 20892, USA

[8] Behavioral Neuroscience Department, Oregon Health and Science University, Portland, OR 97239, USA

[9] Department of Diagnostic Radiology, Yale University School of Medicine, New Haven, CT 06511, USA

[10] Division of Clinical Research, Nathan Kline Institute, Orangeburg, NY 10962, USA

[11] Department of Psychology, University of Wisconsin, Madison, WI 53706, USA

[12] Department of Diagnostic Radiology, Oulu University Hospital, Oulu, Finland

[13] Department of Cognitive Neuroscience, Radboud University Nijmegen Medical Center, The Netherlands

[14] Department of Electrical Engineering and Computer Science, University of Wisconsin-Milwaukee, Milwaukee, WI 53211, USA

[15] Department of Neurology, Lo-Sheng Sanatorium & School of Medicine, National Yang-Ming University, Taiwan

[16] Imaging Institute, The Cleveland Clinic, Cleveland, OH 44195, USA

[17] Brain Imaging and Analysis Center, Duke University Medical Center, Durham, NC, 27710, USA

[18] Max Planck Institute for Human Cognitive and Brain Sciences, Department of Cognitive Neurology, 04103 Leipzig, Germany

[19] Department of Psychiatry and Department of Neurology, Emory University School of Medicine, Atlanta, Georgia 30322, USA

[20] University of Queensland, Brisbane, Queensland, Australia

[21] Department of Psychology, University of Michigan, Ann Arbor MI 48109, USA

[22] Kennedy Krieger Institute, Department of Neuropsychology, Baltimore, MD 21211, USA

[23] F.M. Kirby Research Center for Functional Brain Imaging, Kennedy Krieger Institute, Baltimore, MD 21205, USA

[24] Biomedical Engineering at the University of Michigan, Ann Arbor, MI 48109, USA

[25] McDonnell Center for Higher Brain Functions, Washington University School of Medicine, St. Louis, MO 63110, USA

[26] Department of Neurology, Klinikum Rechts der Isar, Technische Universität München, 81675 Munich, Germany

[27] Leiden Institute for Brain and Cognition (LIBC), Institute for Psychological Research, Leiden University, The Netherlands

[28] Center for BrainHealth & School of Behavioral & Brain Sciences, University of Texas at Dallas, Richardson, TX 75080, USA

[29] Department of Neurology, Washington University School of Medicine, St. Louis, MO 63110, USA

[30] Department of Neurology, Charite University Medical School, Berlin, Germany

[31] Division of Kinesiology, University of Michigan, Ann Arbor, MI 48109-2214, USA

[32] Department of Psychiatry, University of Pittsburgh, Pittsburgh, PA 15213, USA

[33] Department of Psychiatry, Klinikum Rechts der Isar, Technische Universität München, D-81675 Munich, Germany

[34] Jiangsu Key Laboratory of Molecular and Functional Imaging, Department of Radiology, Zhong-Da Hospital, Southeast University, Nanjing 210009, China

[35] Department of Psychiatry, University of Oulu, Oulu 90014, Finland

[36] Berlin NeuroImaging Center and Department of Neurology, Charité Universitaetsmedizin, 10117 Berlin, Germany

[37] Department of Psychiatry, Otto-von-Guericke University of Magdeburg, Magdeburg 39106, Germany

[38] Laboratory for Higher Brain Function, Institute of Psychology, Chinese Academy of Sciences, Beijing 100864, China

[39] Department of Brain and Cognitive Sciences, Harvard-MIT Division of Health Sciences and Technology, Massachusetts Institute of Technology, Boston, MA 02139, USA

[40] Department of Psychiatry, University of Western Ontario, London, ON N6A3H8, Canada

[41] MR Center of Excellence, Medical University of Vienna, 1090 Vienna, Austria

[42] State Key Laboratory of Cognitive Neuroscience and Learning, Beijing Normal University, Beijing 100875, China

Corresponding Author:

Michael P. Milham, Phyllis Green and Randolph Cowen Institute for Pediatric Neuroscience, New York University Child Study Center, NYU Langone Medical Center, 215 Lexington Avenue 14th Floor, New York, NY 10016, USA; Phone: 212-263-2748; Fax: 212-263-4675; Email: michael.milham@nyumc.org

Number of text pages: 13

Number of Figures: 3

Number of Tables: 2 (Table 1 is split into 2 parts upon editorial request)

Abstract

Successfully implemented for exploration of the genome, discovery science has eluded the functional neuroimaging community. The core challenge remains the development of a common paradigm for interrogating the myriad functional systems in the brain without the constraints of a priori hypotheses. Resting-state functional MRI (R-fMRI) constitutes a candidate approach capable of confronting this challenge. Imaging the brain during rest reveals large-amplitude spontaneous low frequency (<0.1 Hz) fluctuations in the fMRI signal that are temporally correlated across functionally related areas. Referred to as functional connectivity, these correlations yield detailed maps of complex neural systems, collectively constituting an individual's functional "connectome." Reproducibility across datasets and individuals suggests the connectome has a common functional architecture. Yet, each individual's connectome exhibits unique features, with stable, meaningful inter-individual differences in connectivity patterns and strengths. Comprehensive mapping of the connectome, and its subsequent exploitation to discern genetic influences and brain-behavior relationships, requires multi-centre collaborative datasets. Here, we initiate this endeavor by gathering R-fMRI data from 1657 volunteers collected independently at 36 international centres. We demonstrate a universal architecture of positive and negative functional connections, as well as consistent loci of inter-individual variability. Age and sex emerged as significant determinants. These results demonstrate that independent R-fMRI datasets can be aggregated and shared. High-throughput R-fMRI can provide quantitative phenotypes for molecular genetic studies and biomarkers of developmental and pathological processes in the brain. To initiate discovery science

for the brain, the “1000 Connectomes” project dataset and all analytical tools referenced in this manuscript will be accessible via www.nitrc.org.

\body

Introduction

Discovery science is data cartography. Much like the challenge of mapping the human genome, the functional neuroimaging community is now facing the complexities of the human connectome. As demonstrated by the 1000 Genomes Project(1), the accumulation and sharing of large-scale datasets for data-mining is central to discovery science.

Although the neuroimaging community has traditionally focused on hypothesis-driven task-based approaches, R-fMRI has recently emerged as a powerful tool for discovery science. Imaging the brain during rest reveals large-amplitude spontaneous low frequency (< 0.1 Hz) fluctuations in the fMRI signal that are temporally correlated across functionally related areas(2-5). A single scan, as brief as 5 minutes, can be used to interrogate simultaneously a multitude of functional circuits, without the constraints of a priori hypotheses. Buttressed by moderate to high test-retest reliability(6), replicability(7, 8) and widespread access, R-fMRI has overcome initial skepticism(9) regarding the validity of examining such an unconstrained state(5, 6, 10). Recent R-fMRI studies have identified putative biomarkers of neuropsychiatric illness(11, 12), provided insights into the development of functional networks in the maturing and aging brain(13-16), demonstrated a shared intrinsic functional architecture(17) between humans and non-human primates(18), and delineated the effects of sleep(19), anesthesia(20) and

pharmacological agents on R-fMRI measures(21, 22). Given the many sources of variability inherent to fMRI, the remaining challenge is to demonstrate the feasibility and utility of adopting a high-throughput model for R-fMRI, commensurate with the scale employed by human genetics studies to have the power to detect both single gene and combinatorial genetic effects on complex phenotypes.

Accordingly, the "1000 Connectomes" project was formed to aggregate existing R-fMRI data from collaborating centers throughout the world and, in so doing, to provide an initial demonstration of the ability to pool functional data across centers. Currently, (September 30, 2009), the repository includes data from 1657 healthy adult participants contributed by 36 laboratories (see Tables 1a and 1b). The intent is to expand this open resource as additional data are made available.

Here, we provide an initial demonstration of the feasibility of pooling R-fMRI datasets across centers. Specifically, we: 1) establish the presence of a universal functional architecture in the brain, consistently detectable across centers, 2) investigate the influence of center on R-fMRI measures, 3) explore the potential impact of demographic variables (age, sex) on R-fMRI measures, and 4) demonstrate an inter-subject variance-based method for identifying putative boundaries between functional networks.

Results

We applied three distinct analytic methods commonly employed in the R-fMRI literature: seed-based functional connectivity, independent component analysis (ICA) and frequency analyses. Across the three methods, we found evidence of: 1) a universal

intrinsic functional architecture in the human brain, 2) center-related variation in R-fMRI measures, and 3) consistent effects of age and sex on R-fMRI measures, detectable across centers despite the presence of center-related variability (see Figure 1). Specifically, seed-based correlational analyses revealed highly consistent patterns of functional connectivity across centers for both the "default mode"(23) and "task-positive" networks(3), supporting a universal functional architecture. Similarly, a data-driven, temporal concatenation ICA approach, combined with dual regression(24-26), revealed consistent patterns of functional connectivity across centers for 20 spatially independent functional networks (see Figure 1 and Supplementary Figure 1). Additionally, for each of the functional connectivity measures, within-site coefficient of variation maps showed a high degree of concordance across centers. This suggests that common loci of variation exist (i.e., centers showed a high degree of agreement on which connections are characterized by relative variance or invariance). Despite the high degree of concordance between centers, there were appreciable center-related variations in the strength of functional connectivity throughout the brain(6). The effect of center was especially prominent in regions exhibiting greater inter-regional connection strength, as they have the least within-center variability. After taking this center-related variability into account, robustly reliable effects of age and sex were appreciable (see Figure 2 and Supplementary Figures 2 and 3). The detection of sex differences was particularly noteworthy, as they are rarely appreciated in the R-fMRI imaging literature. Our findings suggest that this is likely due to modest effect sizes of such sex differences.

In addition to examining patterns of functional connectivity, we measured the amplitude of low frequency fluctuations at each voxel using two common periodogram-

based measures: amplitude of low frequency fluctuation (ALFF; total power < 0.1Hz) (2, 27, 28) and fractional ALFF (fALFF; total power < 0.1Hz / total power in the spectrum)(29). Concordant with prior work, dominance of low frequency fluctuations was consistently noted within gray matter but not white matter regions(29). As with our analyses of functional connectivity, despite clear evidence of center-related effects, we were again able to demonstrate age- and sex-related differences in the magnitude of low frequency fluctuations in a variety of regions, particularly medial wall structures (see Figure 2 and Supplementary Figure 4).

Beyond data-pooling for statistical analysis, we demonstrate the potential to use high-throughput datasets to develop normative maps of functional systems in the brain, which are a prerequisite for clinical applications. Specifically, we exploit a key property of functional connectivity maps—the presence of well-differentiated borders between functionally distinct regions(30). The voxel-wise measures of coefficients of variation for each of the types of functional connectivity maps delineate putative functional boundaries based upon the presence of marked variability in functional connectivity across participants. The variation observed at these boundaries stands in contrast to the low degree of variability observed in regions exhibiting consistently positive or negative connectivity (see Figure 3). Additionally, examination of the coefficients of variation for fALFF measures revealed sharp boundary zones between white and gray matter. It also identified areas of variability in the amplitude of spontaneous fluctuations that coincided with anatomical areas of notable sulcal variability (e.g., cingulate and frontal opercular regions).

Discussion

The present work represents a watershed event in functional imaging: namely, demonstration of the feasibility of pooling and sharing data across multiple centers, alongside the establishment of an open-access data repository. Here we demonstrated: 1) the presence of a universal functional architecture, with remarkable stability in the connectome and its loci of variation across participants and centers, 2) the first evidence of systematic sex differences in R-fMRI measures, as well as age-related gradients even in middle adulthood, and 3) a novel method of highlighting the complex array of putative functional boundaries between networks from which normative maps can be developed. Future work should focus on using the connectome to catalogue phenotypic diversity.

Our results must be considered in light of several limitations. First, we used a convenience sample comprising previously collected data from an array of centers, without prior coordination of acquisition parameters or scanning conditions. While the robustness of our results attests to the consistency of intrinsic brain activity, it still represents a potential underestimate of the true across-center consistency. Our demographic results warrant some caution, as centers were heterogeneous with respect to male-female ratio, mean age and age range. The current findings should motivate more systematic exploration of these variables, as future high-throughput imaging studies will need to take such factors into account. Finally, we applied a limited number of basic analytical approaches. The “1000 Connectomes” project is designed to encourage the development and application of new analytical approaches. For example, future analyses would benefit from taking into account variations in the underlying anatomy in relation to the various aspects of functional connectivity examined here.

All data and analytic tools employed here will be made available via www.nitrc.org as of December 2009. We anticipate that the open availability of the "1000 Connectomes" dataset will recruit the broad participation and collaboration among the scientific community necessary for successful implementation of discovery-based science of human brain function.

Methods

Resting-state fMRI scans were aggregated from 36 community-based datasets (n = 1657). Present analyses were restricted to 24 centers (n = 1093; 21 published, 3 unpublished; mean age below 60; only participants over age 18; 1 scan per participant; duration: 2.2-20 minutes; 970 at 3T; 123 at 1.5T; voxel size: 1.5-5mm within-plane; slice thickness: 3-8mm). Each contributor's respective ethics committee approved submission of de-identified data. The institutional review boards of NYU Langone Medical Center and UMDNJ approved the receipt and dissemination of the data.

For functional connectivity, we used: 1) seed-based correlation analysis based upon 6 previously identified seed regions(31), and 2) model-free independent component analysis (ICA), using temporal concatenation for group analysis and dual regression to generate individual participant maps. For amplitude measures at each voxel, we employed the fast-Fourier transform-based "Amplitude of Low Frequency Fluctuations" (ALFF)(2, 27, 28) and its normalized variant, fractional ALFF (fALFF)(29).

Standard image preprocessing was performed (motion correction, spatial filtering, FWHM = 6 mm, 12-DOF affine transformation to MNI152 stereotactic space). For seed-based correlation approaches and dual-regression following ICA analysis, nuisance

signals (global signal, white matter, cerebrospinal fluid, motion parameters) were regressed out. Temporal filtering was tailored for each analytic approach(22, 24, 29, 31).

ICA components for dual regression analyses were determined by: 1) low-dimensional (20 components) temporal concatenation ICA carried out 25 times (for each, 18 participants were randomly selected from each of 17 centers with minimum 165 time-points), and 2) low-dimensional (20 components) "meta-ICA" – a second concatenation-based ICA using the component sets produced by the 25 runs (see supplementary methods for alternative method). For each participant, dual regression(24-26) was performed using the 20 components identified by the "meta-ICA" (see Supplementary Figure 5), yielding a connectivity map for each component.

Aggregate statistical analyses of center, sex and age effects were based upon a general linear model implementation of one-way ANOVA (factor: center; covariates: age and sex).

To identify functional boundaries we: 1) calculated voxel-wise coefficients of variation across all 1093 participants, and 2) ranked each voxel based on the absolute value of its coefficient of variation.

Acknowledgements

We thank David Kennedy and www.nitrc.org for supporting the "1000 Connectomes" project data release, Avi Snyder for his helpful insights and advice concerning the direction of the project and definition of its goals, and Cameron Craddock for his support of the study. Financial support for the "1000 Connectomes" project was provided by grants to F.X.C. and M.P.M. from the NIMH (R01MH083246), the Stavros S. Niarchos

Foundation, the Leon Levy Foundation, the National Institute on Drug Abuse (1R03DA024775-01) (C.K.), Autism Speaks (M.M.), the Howard Hughes Medical Institute (J.S.A.), and to B.B. from the NIH (R01NS049176), as well as by gifts from Joseph P. Healy, Linda and Richard Schaps, Jill and Bob Smith, and the endowment provided by Phyllis Green and Randolph Cōwen.

References

1. Wise J (2008) Consortium hopes to sequence genome of 1000 volunteers. *British Medical Journal* 336: 237.

2. Biswal B, Yetkin FZ, Haughton VM, Hyde JS (1995) Functional connectivity in the motor cortex of resting human brain using echo-planar MRI. *Magn Reson Med* 34: 537-541.

3. Fox M D, Raichle ME (2007) Spontaneous fluctuations in brain activity observed with functional magnetic resonance imaging. *Nat Rev Neurosci* 8: 700-711.

4. Margulies D S et al (2007) Mapping the functional connectivity of anterior cingulate cortex. *Neuroimage* 37: 579-588.

5. Smith S M et al (2009) Correspondence of the brain's functional architecture during activation and rest. *Proc Natl Acad Sci U S A* 106: 13040-13045.

6. Shehzad Z et al (2009) The resting brain: unconstrained yet reliable. *Cereb Cortex*.

7. He Y et al (2009) Uncovering intrinsic modular organization of spontaneous brain activity in humans. *PLoS ONE* 4: e5226.

8. Buckner R L et al (2009) Cortical hubs revealed by intrinsic functional connectivity: mapping, assessment of stability, and relation to Alzheimer's disease. *J Neurosci* 29: 1860-1873.

9. Morcom A M, Fletcher PC (2007) Does the brain have a baseline? Why we should be resisting a rest. *Neuroimage* 37: 1073-1082.

10. Damoiseaux J S et al (2006) Consistent resting-state networks across healthy subjects. *Proc Natl Acad Sci U S A* 103: 13848-13853.

11. Castellanos F X et al (2008) Cingulate-precuneus interactions: a new locus of dysfunction in adult attention-deficit/hyperactivity disorder. *Biol Psychiatry* 63: 332-337.

12. Church J A et al (2009) Control networks in paediatric Tourette syndrome show immature and anomalous patterns of functional connectivity. *Brain* 132: 225-238.

13. Kelly A M C et al (2009) Development of anterior cingulate functional connectivity from late childhood to early adulthood. *Cereb Cortex* 19: 640-657.

14. Supekar K, Musen M, Menon V (2009) Development of large-scale functional brain networks in children. *PLoS Biol* 7: e1000157.

15. Fair D A et al (2009) Functional brain networks develop from a "local to distributed" organization. *PLoS Comput Biol* 5: e1000381.

16. Andrews-Hanna J R et al (2007) Disruption of large-scale brain systems in advanced aging. *Neuron* 56: 924-935.

17. Hagmann P et al (2008) Mapping the structural core of human cerebral cortex. *PLoS Biol* 6: e159.

18. Vincent J L et al (2007) Intrinsic functional architecture in the anaesthetized monkey brain. *Nature* 447: 83-86.

19. Fukunaga M et al (2006) Large-amplitude, spatially correlated fluctuations in BOLD fMRI signals during extended rest and early sleep stages. *Magn Reson Imaging* 24: 979-992.

20. Greicius M D et al (2008) Persistent default-mode network connectivity during light sedation. *Hum Brain Mapp*.

21. Achard S, Bullmore E (2007) Efficiency and cost of economical brain functional networks. *PLoS Comput Biol* 3: e17.

22. Kelly A M C et al (2009) L-dopa modulates functional connectivity in striatal cognitive and motor networks: a double-blind placebo-controlled study. *J Neurosci* 29: 7364-7378.

23. Gusnard D A, Raichle ME (2001) Searching for a baseline: functional imaging and the resting human brain. *Nat Rev Neurosci* 2: 685-694.

24. Beckmann C F, DeLuca M, Devlin JT, Smith SM (2005) Investigations into resting-state connectivity using independent component analysis. *Philos Trans R Soc Lond B Biol Sci* 360: 1001-1013.

25. Filippini N et al (2009) Distinct patterns of brain activity in young carriers of the APOE-epsilon4 allele. *Proc Natl Acad Sci U S A* 106: 7209-7214.

26. Calhoun V D, Pekar JJ, Pearlson GD (2004) Alcohol intoxication effects on simulated driving: exploring alcohol-dose effects on brain activation using functional MRI. *Neuropsychopharmacology* 29: 2097-17.

27. Zang Y F et al (2007) Altered baseline brain activity in children with ADHD revealed by resting-state functional MRI. *Brain Dev* 29: 83-91.

28. Cordes D et al (2001) Frequencies contributing to functional connectivity in the cerebral cortex in "resting-state" data. *AJNR Am J Neuroradiol* 22: 1326-1333.

29. Zou Q H et al (2008) An improved approach to detection of amplitude of low-frequency fluctuation (ALFF) for resting-state fMRI: fractional ALFF. *J Neurosci Methods* 172: 137-141.

30. Cohen A L et al (2008) Defining functional areas in individual human brains using resting functional connectivity MRI. *Neuroimage* 41: 45-57.

31. Fox M D et al (2005) The human brain is intrinsically organized into dynamic, anticorrelated functional networks. *Proc Natl Acad Sci U S A* 102: 9673-9678.

Figure Legends

Fig. 1. **Independent Site, Age- and Sex-Related Variations Detected in R-fMRI Measures of Functional Connectivity and Amplitude Fluctuation**.

The first row depicts group-level maps for representative seed-based (column 1) and ICA-based (column 3) functional connectivity analyses (see supplementary materials for complete results), as well as fractional amplitude of low frequency fluctuations (fALFF; column 2). Group-level maps were derived from one-way ANOVA across 1093 participants from 24 centres (factor: center; covariates: age and sex). All group-level maps depicted were corrected for multiple comparisons at the cluster-level using gaussian random field theory ($Z > 2.3$, $p < .05$, corrected). For each measure, the second row shows robust between-center concordances (Kendall's W), with the voxel-wise coefficients of variation above the diagonal and the voxel-wise means below. Rows 3, 4 and 5 depict voxels exhibiting significant effects of center, age and sex as detected by the one-way ANOVA. PCC = posterior cingulate cortex; seed region indicated by white dot; IC13 = independent component 13. Top left: surface map legend. LL = Left Lateral surface; RL = Right Lateral; LM = Left Medial; RM = Right Medial. All surface maps are rendered on the PALS-B12 atlas in CARET (http://brainvis.wustl.edu).

Fig. 2. Illustrative Areas Exhibiting Age- and Sex-Related Variation in R-fMRI Properties.

Significant group-level variance in functional connectivity maps was explained by age and sex (cluster-based Gaussian random field corrected: $Z > 2.3$, $p < .05$). For each of three methods (seed-based, fALFF, ICA), variance in connectivity strength explained by

age (left) and sex (right) is illustrated both anatomically and graphically. Age-related differences are represented as scatterplots. Sex-related differences are represented as histograms depicting the distributions of RSFC values for males and females separately. Vertical lines indicate peak values. Corresponding topographical brain areas are indicated by arrows. PCC = posterior cingulate cortex; fALFF = fractional amplitude of low frequency fluctuations; ICA = Independent Component Analysis; IC13 = independent component 13. RSFC = resting-state functional connectivity.

Fig. 3. Variation Across Individuals Reveal Functional Boundaries.

Previous work has noted that functionally segregated regions are frequently characterized by well-demarcated boundaries for an individual(30). As such, variability in boundary areas is detectable across participants. Here we detect functional boundaries via examination of voxel-wise coefficients of variation (absolute value) for fALFF and selected seed-based (IPS, PCC) and ICA-based (IC13) functional connectivity maps. For the purpose of visualization, coefficients of variation were rank-ordered, whereby the relative degree of variation across participants at a given voxel, rather than the actual value, was plotted to provide a better contrast of brain regions. Ranking coefficients of variation efficiently identified regions of greatest inter-individual variability thus delineating putative functional boundaries.

Table Legends

Table 1a. Data currently included in the '1000 Connectomes' project

[1] Actual number of participants included in the analysis, if different from N

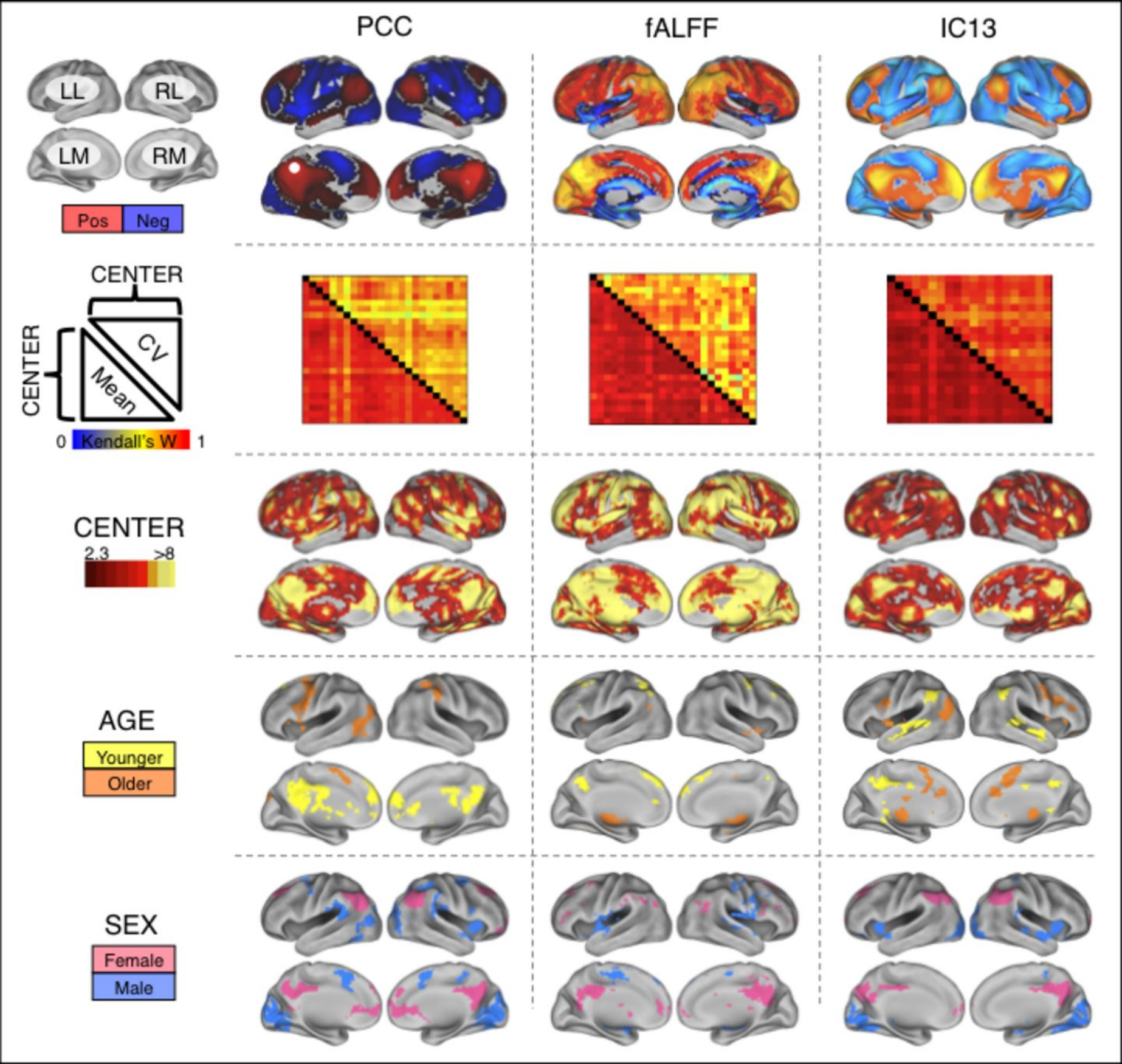
Table 1b. Data currently included in the '1000 Connectomes' project

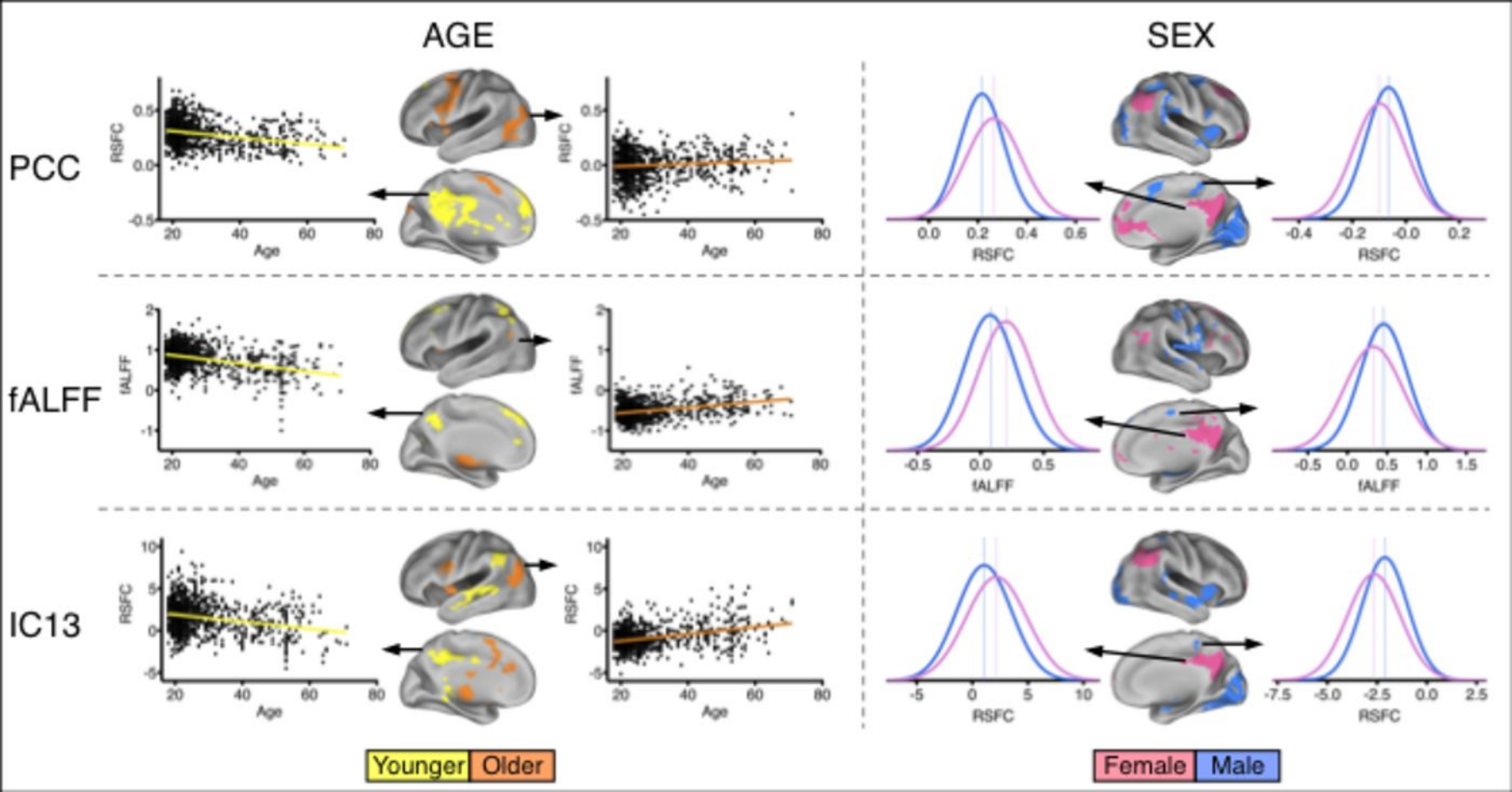
[1] Actual number of participants included in the analysis, if different from N

[2] Data from same magnet, different sequence

[3] 1.5T Magnet

* The following data will be included in the '1000 Connectomes' data release but are not included in the current analyses: Ann Arbor, MI, USA, Christopher S. Monk/Rachael D. Seidler/Scott J. Peltier; Atlanta, GA, USA, Helen S. Mayberg; Berlin, Germany, Sein Smidt; Durham, NC, USA, David J. Madden; Durham, NC, USA, Lihong Wang; London, Ontario, Canada, Peter Williamson; Munchen, Germany, Christian Sorg/Valentin Riedl; Nanjing, China, Gao-Jun Teng/Hong-Ying Zhang[3]; Pittsburgh, PA, USA, Greg Siegle; Portland, OR, USA, Damien Fair; Taipei, Taiwan, Ching-Po Lin; Vienna, Austria, Christian Windischberger


PCC
fALFF
IC13
LL
RL
LM
RM
Pos
Neg
CENTER
CENTER
CV
Mean
0
Kendall's W
1
CENTER
2.3
>8
AGE
Younger
Older
SEX
Female
Male


AGE
SEX
PCC
fALFF
IC13
RSFC
fALFF
Age
Younger
Older
Female
Male

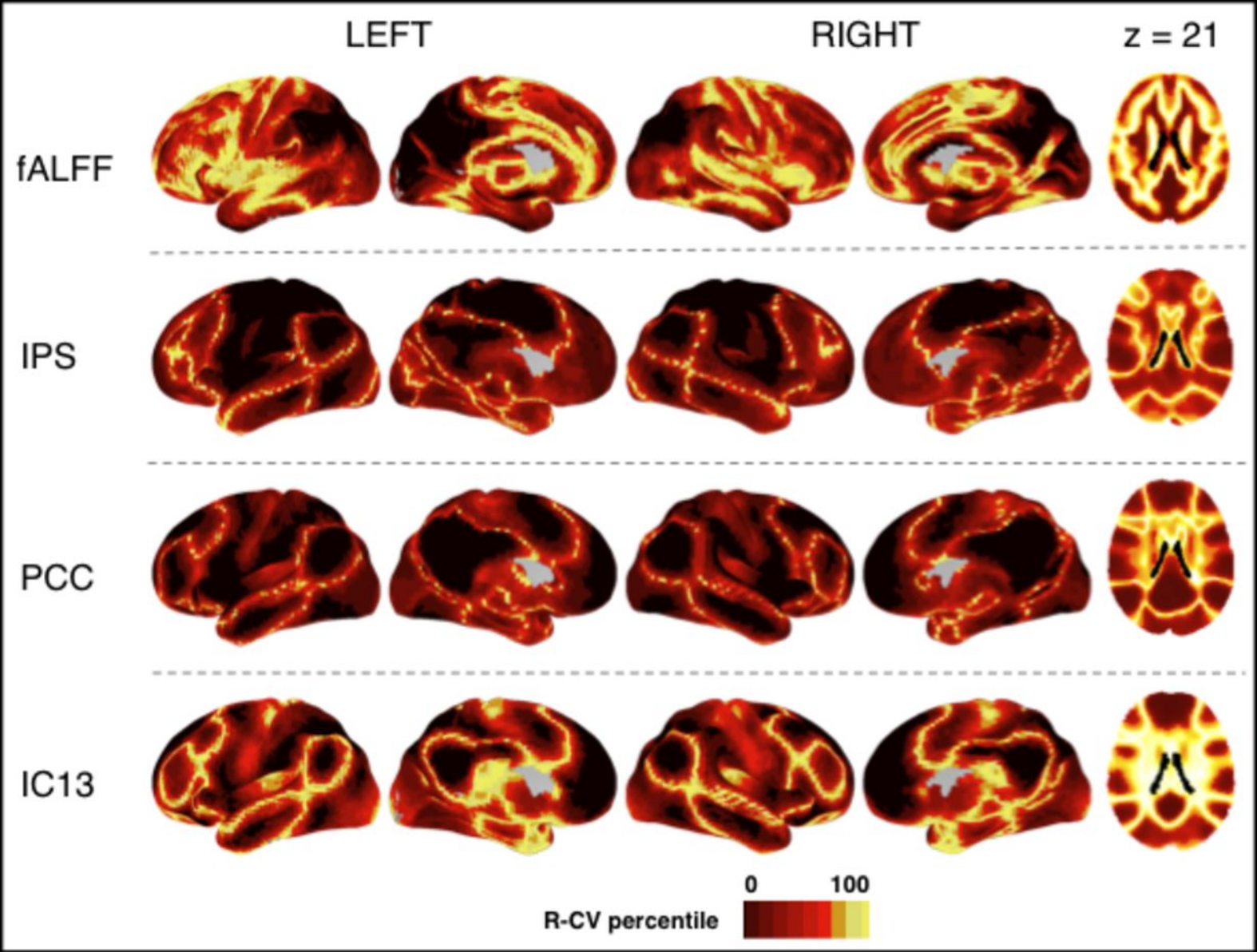

LEFT
RIGHT
z = 21
fALFF
IPS
PCC
IC13
0
100
R-CV percentile

Table 1a. Data currently included in the '1000 Connectomes' project

	Center	*PI*	*N*	*n*[1]	*Age*	*Age range*	*Sex (% males)*
1.	Baltimore, MD, USA	James J. Pekar/Stewart H. Mostofsky	23		29.26 (5.46)	20-40	35%
2.	Bangor, UK	Stan Colcombe	20		23.4 (5.32)	19-38	100%
3.	Beijing, China	Yu-Feng Zang	198	193	21.16 (1.83)	18-26	39%
4.	Beijing, China	Xu-Chu Weng	28	27	20.41 (1.39)	18-24	27%
5.	Berlin, Germany	Daniel Margulies	26		29.77 (5.21)	23-44	50%
6.	Bethesda, MD, USA	Monique Ernst	18		33.00 (13.31)	18-53	22%
7.	Cambridge, MA, USA	Randy L. Buckner	198		21.03 (2.31)	18-30	38%
8.	Cambridge, MA, USA	Susan Whitfield-Gabrieli	39	35	25.09 (3.53)	20-32	49%
9.	Cleveland, OH, USA	Mark J. Lowe	31		43.55 (11.14)	24-60	35%
10.	Dallas, TX, USA	Bart Rypma	24		42.63 (20.07)	20-71	50%
11.	Hvidovre, Denmark	Anne-Marie Dogonowski/Kristoffer Madsen	28		41.75 (10.7)	21-68	50%
12.	Leiden, Netherlands	Serge A.R.B. Rombouts	31		22.19 (2.57)	18-28	74%
13.	Leipzig, Germany	Arno Villringer	37		26.22 (5)	20-42	43%
14.	Magdeburg, Germany	Martin Walter	29	28	30.43 (5.71)	22-43	93%
15.	Milwaukee, WI, USA	Shi-Jiang Li	64		53.59 (5.79)	44-65	64%
16.	New Haven, CT, USA	Michelle Hampson	19	18	31.61 (10.27)	18-48	56%

Table 1b. Data currently included in the '1000 Connectomes' project.

	Center	*PI*	*N*	*n*[1]	*Age*	*Age range*	*Sex (% males)*
17.	New York City, NY, USA[2]	Michael Milham/F. Xavier Castellanos	59		32.78 (8.83)	20-49	68%
18.	New York City, NY, USA[2]	Michael Milham/F. Xavier Castellanos	20		29.75 (9.94)	18-46	40%
19.	Newark, NJ, USA	Bharat B. Biswal	19		24.11 (3.91)	21-39	47%
20.	Orangeburg, NY, USA[3]	Matthew J. Hoptman	22	20	40.65 (11.03)	20-55	75%
21.	Oulu, Finland[3]	Vesa J. Kiviniemi/Juha Veijola	103		21.52 (0.57)	20-23	36%
22.	Oxford, UK	Steve M. Smith/Clare Mackay	22		29 (3.79)	20-35	55%
23.	Queensland, Australia	Katie McMahon	19	18	26.28 (3.71)	20-35	61%
24.	Saint Louis, MO, USA	Bradley L. Schlaggar/Steven E. Petersen	31		25.1 (2.31)	21-29	45%